Inorganic Chemistry

Article

pubs.acs.org/IC

Ambient Stable Trigonal Bipyramidal Copper(III) Complexes Equipped with an Exchangeable Axial Ligand

Hao-Ching Chang,[†] Feng-Chun Lo,[§] Wen-Chi Liu,[†] Tsung-Han Lin,[†] Wen-Feng Liaw,[§] Ting-Shen Kuo,[‡] and Way-Zen Lee*[,†]

[†]Department of Chemistry and [‡]Instrumentation Center, National Taiwan Normal University, Taipei 11677, Taiwan

[§]Department of Chemistry, National Tsing Hua University, Hsinchu 30013, Taiwan

Supporting Information

ABSTRACT: A stable trigonal bipyramidal copper(III) complex, [PPN][Cu(^{TMS}PS3)Cl] (**1**, wherein PPN represents bis(triphenylphosphine)iminium), was synthesized from $CuCl_2$/PPNCl via intramolecular copper(II) disproportionation. Under ambient conditions, the axial chloride of **1** is exchangeable in solution thus making **1** serve as an intermediate to prepare trigonal bipyramidal copper(III) derivatives, e.g., [PPN][Cu(^{TMS}PS3)(N_3)] (**2**) and [Cu(^{TMS}PS3)(DABCO)] (**3**). Diamagnetic complexes **1**−**3** were fully characterized by X-ray crystallography, NMR, UV−vis, and Cu K-edge absorption spectroscopy. A series of UV−vis titrations were performed to investigate the relative ligand affinity toward the [Cu(^{TMS}PS3)] moiety, verifying the 1:1 binding equilibrium between various ligands. Compared to known copper(III) compounds, Cu K-edge absorptions of **1**−**3** possess lower pre-edge energy and higher shakedown transition energy, which, respectively, attribute to the electron donation from $^{TMS}PS3^{3-}$ ligand and their trigonal ligand field.

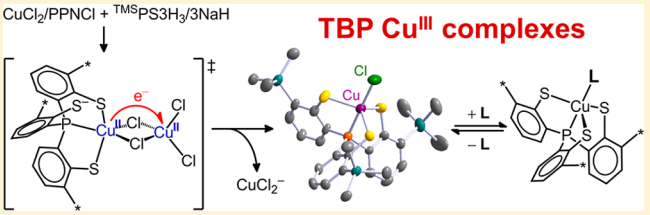

INTRODUCTION

Trivalent copper species participate in various chemical processes.[1−3] Over the past decades, activation of dioxygen by copper(I) species to form dinuclear copper(III) bis(μ-oxo) complexes has been well-established.[4,5] Recently, several mononuclear Cu−O_2 adducts were characterized at low temperature.[6−8] Copper(III)-peroxo complexes stabilized by sterically hindered bidentate ligands (Scheme 1, type B)[6] and copper(II)-superoxo complexes supported by tripodal ligands[7,8] reveal that the supporting ligand governs the electronic structure and reactivity of copper species.[9] Importantly, organocopper(III) species have been identified as the key intermediate in many cross-coupling reactions and C−H bond activations.[1−3,10−14] Structural evidence for the copper(III) intermediate of cross-coupling reactions and C−H bond activations has been demonstrated by the studies of the aryl copper(III) complexes with triazamacrocyclic ligands.[13,14] To date, most of the structurally characterized copper(III) complexes possess tetragonal geometry;[1,12−18] only two of them are trigonal bipyramidal (TBP): [Cu(tptm)Cl][PF_6] was chemically oxidized from its copper(II) precursor,[19] and (bpy)Cu(CF_3)$_3$ was prepared from the homoleptic [Cu(CF_3)$_4$]$^-$ anion very recently.[20] Despite the formation of copper(III) complexes having been reported, the chemistry of trivalent copper species remains less explored.

Scheme 1. Types of Reactions Forming Mononuclear Copper(III) Compounds

A. Conventional oxidation from copper(II)

LCu^{II} —oxidant→ LCu^{III} ref. 19

B. Oxygenation with copper(I)

LCu^{I} —O_2→ $LCu^{III}(O_2)$ ref. 6

C. Disproportionation of copper(II)

$LCu^{II} + (L)Cu^{II}$ —e⁻ transfer→ $LCu^{III} + (L)Cu^{I}$ ref. 13,14,25

$L^{3-} + [Cu^{II}_2Cl_6]^{2-}$ —e⁻ transfer→ $[LCu^{III}Cl]^- + [Cu^{I}Cl_2]^- + 3\ Cl^-$

Deprotonated 2,2′,2″-trimercapto-3,3′,3″-tris(trimethylsilyl)-triphenylphosphine ($^{TMS}PS3H_3$)[21] is a promising chelator to stabilize various high valent metal ions, e.g., vanadium(III),[22] manganese(IV),[23] iron(IV),[24] and nickel(III).[25] We herein demonstrate a synthetic approach for trigonal bipyramidal copper(III) complexes through an isolable chloride-bound intermediate, [PPN][Cu(^{TMS}PS3)(Cl)] (**1**, Figure 1, wherein PPN represents bis(triphenylphosphine)iminium), prepared via copper(II) disproportionation triggered by the $^{TMS}PS3^{3-}$ ligand (Scheme 1, type C).

RESULTS AND DISCUSSION

Preparation and Proposed Mechanism of Complex 1.

Synthesis of **1** was carried out in THF/CH_3CN mixed solvent by the reaction of the deprotonated $^{TMS}PS3^{3-}$ ligand with a $CuCl_2$/PPNCl mixture in a 1:1:1 molar ratio (details in Experimental Section). Actually, with 1 equiv of PPNCl, polymeric $CuCl_2$ is converted to soluble [PPN]$_2$[Cu_2Cl_6] in CH_3CN.[26] Upon addition of $^{TMS}PS3^{3-}$ ligand into [Cu_2Cl_6]$^{2-}$

Received: March 16, 2015
Published: May 20, 2015

DOI: 10.1021/acs.inorgchem.5b00603
Inorg. Chem. 2015, 54, 5527−5533

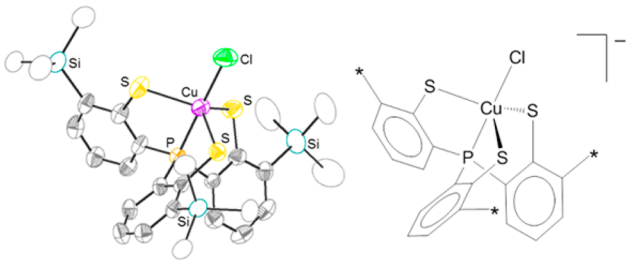

Figure 1. Drawings of **1**: ORTEP at 50% probability (left) and schematic representation (right). Counterion and hydrogen atoms are omitted for clarity. Asterisk (*) represents TMS groups of the $^{TMS}PS_3^{3-}$ ligand. Selected bond distances (Å) and angles (deg): Cu−P, 2.1279(16); Cu−S1, 2.3477(23); Cu−S2, 2.3734(23); Cu−S3, 2.3436(29); Cu−Cl, 2.2011(18); P−Cu−Cl, 179.074(85); S1−Cu−S2, 117.326(75); S1−Cu−S3, 121.189(89); S2−Cu−S3, 112.421(80).

solution, the resulting solution turned deep purple immediately. After removal of brown and off-white precipitate, dark purple crystals of **1** were obtained by vapor diffusion of Et_2O into CH_2Cl_2 solution of **1** under −10 °C (32% yield, Table 1, entry 1). Colorless crystals of $[PPN][CuCl_2]$ characterized by X-ray crystallography were also obtained from the crude mixture, disclosing that part of the copper(II) species was reduced. Moreover, the yield of **1** from the $CuCl_2$/PPNCl mixture was improved up to 44% by bubbling O_2 into the reaction solution (Table 1, entry 2), implying recycling of copper(I) species. Meanwhile, $[PPN][CuCl_2]$ was in situ oxidized and reacted with $^{TMS}PS3^{3-}$ ligand under oxygenated solution to give a comparable yield of **1** (Table 1, entry 3). In addition, utilizing $[PPN]_2[Cu_2Cl_6]$ to react with $^{TMS}PS3^{3-}$ without O_2 also produced **1** (Table 1, entry 4) indicating that the dinuclear $[Cu_2Cl_6]^{2-}$ is the active species. The formation of **1** and $[PPN][CuCl_2]$ suggests an intramolecular disproportionation mechanism. No intermediate, however, was observed as the deprotonated ligand was reacted with $[PPN]_2[Cu_2Cl_6]$, even at −80 °C. A ligand-bound dinuclear species, proposed as $[(^{TMS}PS3)Cu^{II}(\mu\text{-}Cl)_2Cu^{II}(Cl)_2]^{3-}$ (depicted in Scheme 2), should correspond to an inner sphere electron transfer, triggered by highly electron-donating $^{TMS}PS3^{3-}$ ligand, to form trivalent **1**. During the electron transfer, the distal copper(II) ion is simultaneously reduced and dissociated to yield the copper(I) byproduct. Although few examples of disproportionation of copper(II) have been reported,[13,14,27] none of these provided evidence of inner sphere electron transfer.

Table 1. Yield of 1 by Different Preparation Conditions

entry	Cu source	additive	O_2	yield of **1**[a]
1	$CuCl_2$	PPNCl	−	32 ± 3%
2	$CuCl_2$	PPNCl	+	44 ± 2%
3	$[PPN][CuCl_2]$		+	39 ± 3%
4	$[PPN]_2[Cu_2Cl_6]$		−	33 ± 5%

[a]The crystal yield was measured by signal integration in ^1H NMR with NEt_4BF_4 as internal standard.

Scheme 2. Proposed Mechanism of the Formation of 1[a]

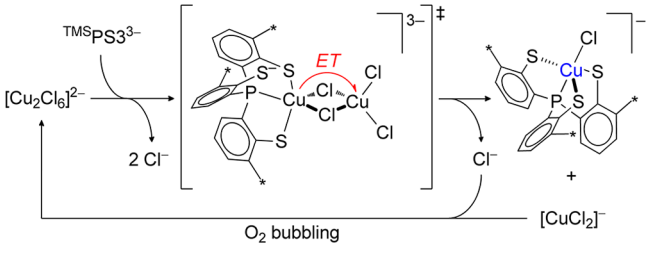

[a]Asterisk (*) represents TMS groups of the $^{TMS}PS3^{3-}$ ligand.

Structural Characterization of Complex 1. The X-ray structure of **1** reveals that the copper center is coordinated by the trianionic $^{TMS}PS3^{3-}$ ligand and a Cl^- ion. The nearly perfect TBP geometry of **1** (τ_5 = 0.96) indicates a low spin d^8 configuration without Jahn−Teller distortion, whereas the nickel derivative, $[PPN][Ni^{III}(^{TMS}PS3)Cl]$, has a distorted TBP structure (τ_5 = 0.70).[25a] The EPR spectra of **1** are silent either at 77 K or at room temperature (Supporting Information Figure S3), revealing no low lying triplet excited state exists. This diamagnetism is consistent with density functional theory (DFT) calculations,[28] supporting a trivalent copper held in TBP geometry: the lowest unoccupied molecular orbital (LUMO) of **1** has great d_{z^2} character while lower ones accommodate valence electrons in d^8 configuration (Figure 2).

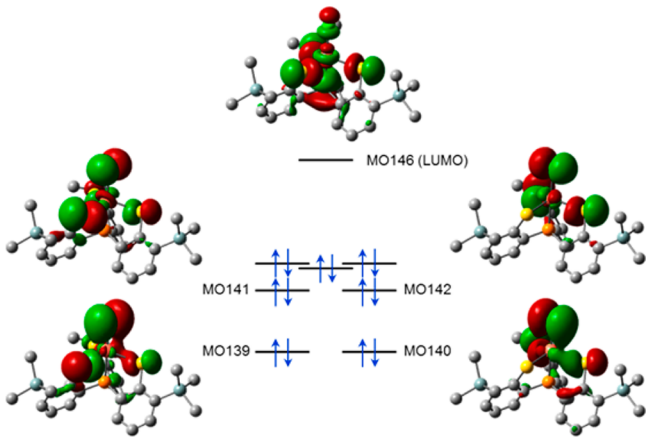

Figure 2. Frontier orbitals of **1** form DFT calculation. Orbitals with recognizable 3d character are represented by surfaces of 0.03 isovalue.

The intense purple color of **1** is mainly attributed to its 525 nm absorption band, together with another moderate absorption at 730 nm (Figure 3a). As suggested by TD-DFT calculations, both transitions are assigned as intramolecular charge transfer to the LUMO (Figure 3b).

As the UV−vis absorption of **1** in CH_3CN is monitored, a shoulder would gradually emerge around 470 nm; the pattern change is even faster in less polar solvents, i.e., CH_2Cl_2, THF. When taking a ^1H NMR spectrum of **1**, two similar sets of signals were exhibited. The minor species was suppressed by adding excess PPNCl and considered as a copper(III) species. This behavior differs from that of $[Cu(tptm)Cl][PF_6]$, which converts into an EPR-active pseudo-octahedral species by adding excess Cl^- ion.[19] The axial chloride of **1** partially dissociates in CH_3CN, although crystalline **1** is stable under air. The phenomenon was confirmed by high resolution ESI-MS (Supporting Information Figure S8a). Encouraged by these observations, investigation of ligand exchange with various N-donors was processed. Since the LUMO of **1** has discernible d_{z^2} orbital contribution, its energy level is correlated to the axial ligand-field. The charge transfer bands would hence shift with

DOI: 10.1021/acs.inorgchem.5b00603
Inorg. Chem. 2015, 54, 5527−5533

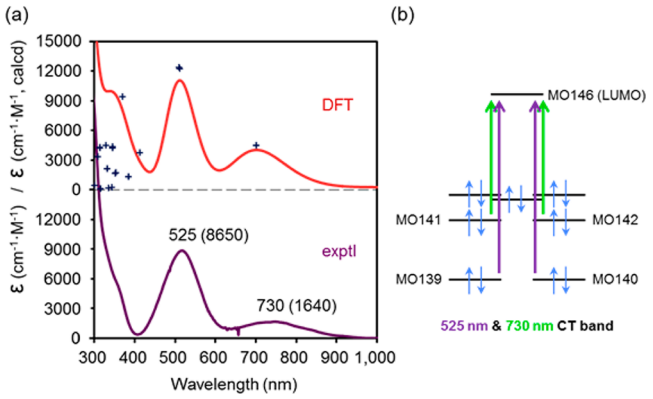

Figure 3. (a) UV−vis spectra of **1** calculated by TD-DFT (top) and measured in CH_3CN solution (bottom). The simulated spectrum is composed by the first 60 transitions, of which oscillators are labeled (+). (b) DFT-calculated transitions corresponding to the main charge transfer bands.

the variation of the axial ligand, whereby the ligand exchange with **1** can be studied by UV−vis spectroscopy.

Ligand Exchange on $Cu^{III}(^{TMS}PS3)$ Moiety. For an understanding of the transformation of **1** in solution, ligand titrations of **1** were conducted in a competitive mode with additional PPNCl. Analysis of UV−vis titration shows that the $Cu(^{TMS}PS3)$−ligand interaction complies with 1:1 binding equilibrium, shown as Figure 4 (details in the Experimental Section). The quantified ligand affinity toward the $Cu(^{TMS}PS3)$ moiety (Table 2) is acquired by fitting of titration isotherms. Those exchanges completed within several minutes under room temperature, implying the hemilability of the axial ligand.

Interestingly, chloride substitution of **1** occurs not only with anionic ligands but also with neutral N-donors, such as 1,4-diazabicyclo[2.2.2]octane (DABCO), *N*-methylimidazole (*N*-MeIm), and pyridines. In this scope, N_3^- has the highest binding affinity but it is not much different from that of DABCO and *N*-MeIm, of which ΔG_{ex}° values are less than 3 kJ/mol. This finding epitomizes the observation that it is not Coulombic interaction but likely nucleophilicity of ligand that governs the $[Cu(^{TMS}PS3)]$−ligand interaction. Namely, the electron density of the copper(III) center is compensated by the $^{TMS}PS3^{3-}$ ligand. Compared with pyridine, the steric factor takes place leading an affinity drop by 2 orders of magnitude for 2,6-lutidine (ca. 12 kJ/mol in ΔG_{ex}°). Notably, these exchanges with weaker ligands unequivocally occur also providing evidence that the apical ligand should dissociate in solution forming a solvent-associated species. Besides, exchange between **1** and [PPN]SCN is sluggish, correlating to the inferior affinity of such an ambidentate ligand.

Derivatization from Chloride-Bound Intermediate. On the basis of the ligand exchange results, complex **1** was employed as a precursor to generate other TBP copper(III) complexes under ambient conditions. Reaction of **1** with excess NaN_3 yielded complex $[PPN][Cu(^{TMS}PS3)(N_3)]$ (**2**, Figure 5a). Complex **2** can also be synthesized in situ from a one-pot reaction by subsequent addition of NaN_3 into the preparation solution of **1**. Presumably, precipitation of NaCl drives the reaction to the N_3-bound complex **2**. In a similar fashion, neutral DABCO-bound $[Cu(^{TMS}PS3)(DABCO)]$ (**3**, Figure 5b) was prepared by adding excess DABCO to the CH_3CN solution of **1**. The X-ray structures of **2** and **3** show the copper center remaining in nearly perfect TBP geometry (τ_5 = 0.98 for **2**, 0.97 for **3**). Crystallographic data are listed in Table 3. In contrast, reaction of **1** with NaSCN yielded a mixture of $[Cu(^{TMS}PS3)(SCN)]^-$ and **1** which cocrystallized in the lattice (see the Experimental Section). All these conversions are represented in Scheme 3.

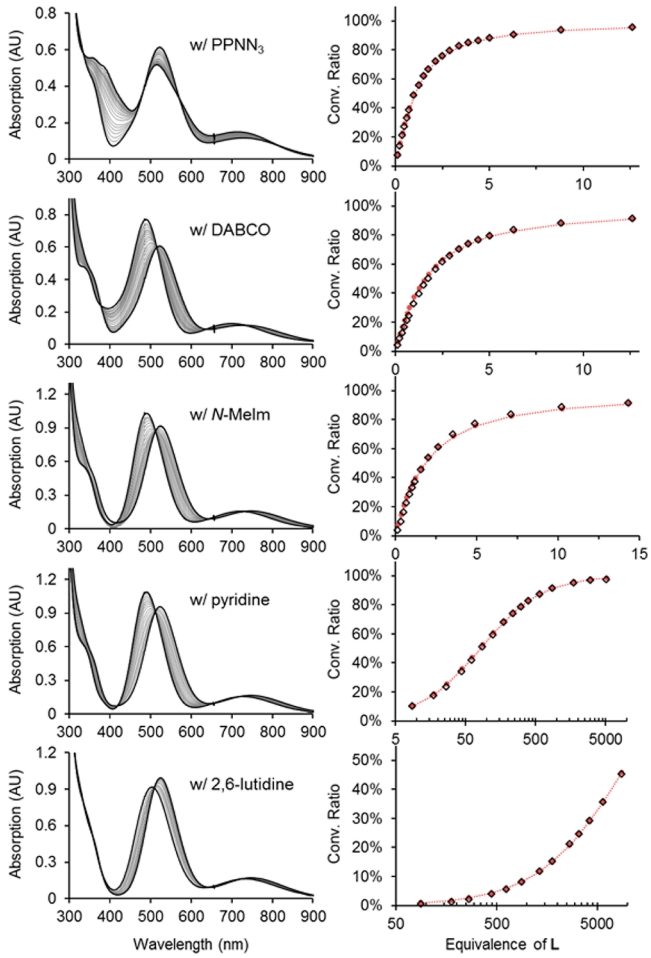

Figure 4. UV−vis titrations and fitting with various incoming ligands.

Table 2. Relative Ligand Affinity toward the $Cu(^{TMS}PS3)$ Moiety

ligand	K_{ex}[a]	ΔG_{ex}° (kJ/mol)
N_3^-	18(1)	−7.2
DABCO[b]	8(1)	−5.2
N-MeIm[b]	7(1)	−4.8
pyridine	0.13(1)	+5.0
2,6-lutidine	0.0010(1)	+17

[a]Equilibrium constants of various ligands are referenced by chloride-bound **1**. [b]Abbreviations: DABCO = 1,4-diazabicyclo[2.2.2]octane; *N*-MeIm = *N*-methylimidazole.

X-ray Absorption Spectra of 1−3. X-ray absorption near-edge structure (XANES) unveils the local electronic environment of an irradiated metal/element, and the Cu K-edge transitions in different oxidation states have been systematically discussed.[29] Since the $^{TMS}PS3^{3-}$-bound copper(II) species was not obtained, $[PPN]_2[Cu_2Cl_6]$ with soft chloride ligands was chosen as a reference. Cu K-edge absorption spectra of crystalline powder of **1**−**3** (Figure 6) were measured in transmission mode. Deconvolution of the obtained spectra reveals the implicit pre-edge (1s → 3d) transitions of **1**−**3**

DOI: 10.1021/acs.inorgchem.5b00603
Inorg. Chem. 2015, 54, 5527−5533

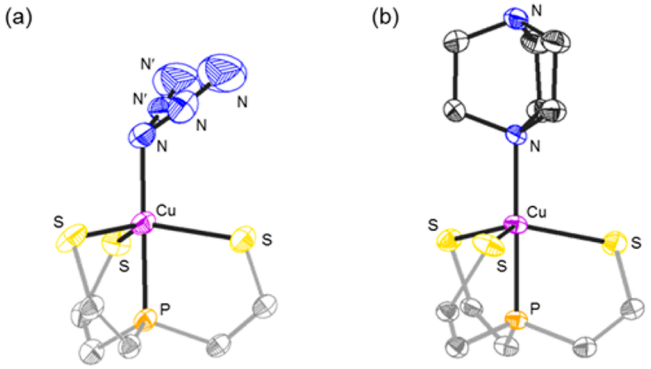

Figure 5. ORTEP drawings of the coordination around the copper(III) center in **2** (a) and **3** (b) at 50% probability. TMS groups, part of phenyl rings of **2** and **3**, counterion of **2** and all hydrogen atoms are omitted for clarity. Selected bond distances (Å) and angles (deg) of **2**: Cu−P, 2.1391(11); Cu−S1, 2.3181(12); Cu−S2, 2.3525(17); Cu−S3, 2.3405(14); Cu−N1, 1.9297(34); P−Cu−N1, 179.186(113); S1−Cu−S2, 120.388(53); S1−Cu−S3, 119.006(50); S2−Cu−S3, 113.087(52). Selected bond distances (Å) and angles (deg) of **3**: Cu−P, 2.1465(6); Cu−S1, 2.3298(10); Cu−S2, 2.3390(8); Cu−S3, 2.3421(8); Cu−N1, 2.0081(16); P−Cu−N1, 179.271(63); S1−Cu−S2, 120.827(28); S1−Cu−S3, 116.650(32); S2−Cu−S3, 113.413(29).

centered around 8980.5 eV (Figure 6, inset, and Table 4) with a ~2 eV shift from $[PPN]_2[Cu_2Cl_6]$ (8978.7 eV). The pre-edge energies of **1**−**3** are slightly lower than those of the known copper(III) species (8981.0 ± 0.5 eV).[9a,13a,29c] The relatively lower pre-edge energies of **1**−**3** agree that the copper(III) center of **1**−**3** was compensated by the electron-donating $^{TMS}PS3^{3-}$ ligand. The rising edge of **1**−**3** has a significant contribution from 1s → 4p transitions. The shoulder of edge jump is attributed to the shakedown transition (1s → 4p + LMCT),[29a] summarized in Table 4. Complexes **1**−**3** having higher shakedown energies than those in tetragonal complexes[29,30] are due to the elevated $4p_z$ orbital of the copper(III) center[31] in the TBP ligand field of **1**−**3**.

Scheme 3. Transformations of $[Cu^{III}(^{TMS}PS3)(L)]^{-/0}$ Species in CH_3CN Solution[a]

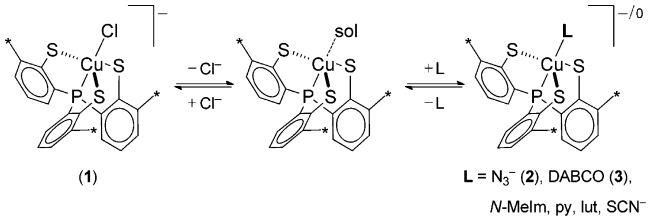

[a]Abbreviations: DABCO = 1,4-diazabicyclo[2.2.2]octane; *N*-MeIm = *N*-methylimidazole; py = pyridine; lut =2,6-lutidine.

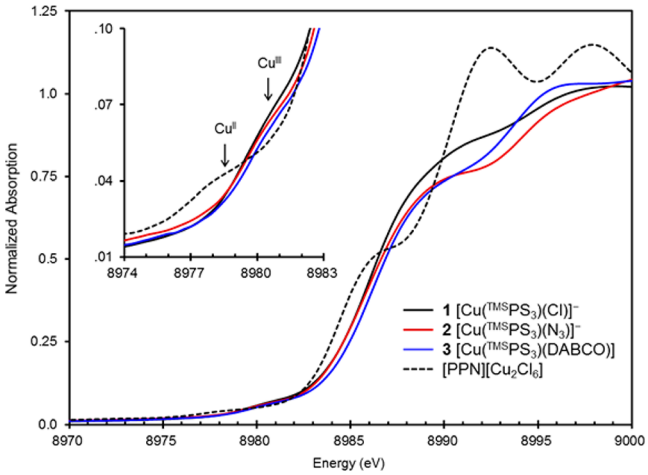

Figure 6. Cu K-edge absorption of **1** (black), **2** (red), **3** (blue), and $[PPN]_2[Cu_2Cl_6]$ (dashed line). Spectra were calibrated with the first inflection point of Cu foil absorption set at 8980.3 eV. The inset shows the amplified pre-edge region.

EXPERIMENTAL SECTION

Materials and Instrumentation. Synthesis of 2,2′,2″-trimercapto-3,3′,3″-tris(trimethylsilyl)triphenylphosphine ($^{TMS}PS3H_3$)[21] ligand and its complexation with copper ion were performed under nitrogen atmosphere using standard Schlenk and glovebox techniques. Crystallization and manipulations with complexes were processed

Table 3. Crystallographic Data for 1−3

	1	2	3
formula	$C_{127}H_{134}Cl_4Cu_2N_2P_6S_6Si_6$	$C_{63.5}H_{67}ClCuN_4P_3S_3Si_3$	$C_{72}H_{102}Cu_2N_4P_2S_6Si_6$
fw	2503.96	1258.56	1573.50
space group	$P\bar{1}$	$P\bar{1}$	$P\bar{1}$
a (Å)	11.4117(5)	14.7323(10)	10.0970(4)
b (Å)	15.4422(6)	15.1200(14)	15.1624(6)
c (Å)	21.9728(9)	18.1122(16)	15.3101(7)
α (deg)	98.225(2)	75.436(4)	110.765(2)
β (deg)	98.850(3)	83.822(4)	98.845(2)
γ (deg)	110.687(3)	66.337(4)	105.154(2)
V (Å^3)	3496.7(2)	3576.5(5)	2035.04(15)
Z	1	2	1
T (K)	200(2)	200(2)	200(2)
λ (Å)	0.710 73	0.710 73	0.710 73
D_{calcd} (g cm^{-3})	1.189	1.169	1.284
μ (mm^{-1})	0.634	0.585	0.845
R1[a]/wR2[b] [$I > 2\sigma(I)$]	0.0783/0.1916	0.0620/0.1745	0.0363/0.0874
R1[a]/wR2[b] (all data)	0.1630/0.2198	0.0888/0.1894	0.0535/0.0958

[a]$R1 = \sum||F_o| - |F_c||/\sum|F_o|$. [b]$wR2 = (\sum w(F_o^2-F_c^2)^2/\sum w(F_o^2)^2)^{1/2}$.

DOI: 10.1021/acs.inorgchem.5b00603
Inorg. Chem. 2015, 54, 5527−5533

Table 4. Energy of Cu K-Edge Transitions of Copper(III) Species

Cu^{III} species[a]	pre-edge[b]	1s → 4p + LMCT[b]	ref
1	8980.4	8987.5	this work
2	8980.6	8987.9	this work
3	8980.5	8987.9	this work
$[(L^{iPr})Cu^{III}(O_2)]$	8980.7	8986.5	9a
$[(L_{ME}Cu^{III})_2(\mu\text{-}O)_2]^{2+}$	8980.9	8987.1	29c
$[Cu^{III}(H23m)]^{2+}$	8981.2		13b
$[Cu^{III}(MNT)_2]^-$	8980.7	8986.6	30

[a]Abbreviations: L^{iPr} = 2,4-bis(2,6-diisopropylphenylimido)-3-pentyl; L_{ME} = 1,2-bis(ethylmethylamino)cyclohexane; H23m = 1,8-(1,3-phenylene-bis(methylene))-1,4,8-triaza-octane; MNT = maleonitrile-dithiolate. [b]Energies are denoted in eV unit.

under air. Tetrahydrofuran (THF) was distilled from sodium/benzophenone under nitrogen atmosphere; CH_3CN, CH_2Cl_2, Et_2O, and hexanes were purified by MBraun Solvent Purification System (MB-SPS). Dimeric $[PPN]_2[Cu_2Cl_6]$[26] was prepared according to published method. $[PPN]N_3$ and [PPN]SCN for titration were prepared by counterion exchange from their sodium salt with PPNCl, and recrystallized prior to usage. Other chemical reagents were obtained from commercial sources and used as received. Nuclear magnetic resonance spectra were recorded on Bruker Avance-400 MHz NMR spectrometers. UV−vis spectra were recorded with an Agilent 8453 spectrophotometer. Infrared spectra were measured by a PerkinElmer Paragon 500 FT-IR spectrometer. High resolution electrospray mass spectra were recorded by an AB SCIEX QSTAR XL system. Elemental analysis was performed on an elementar Vario EL cube analyzer at the Instrumentation Center in National Taiwan University. For X-ray structural analysis, crystals of **1**−**3** were selected under a microscope. Diffraction data were collected on a Bruker-Nonius Kappa CCD diffractometer employing Mo Kα radiation (λ = 0.7107 Å) at 200 K and with a θ−2θ scan mode. The space groups were determined on the basis of systematic absences and intensity statistics. The structures of **1**−**3** were solved by direct methods using SIR92 or SIR97, and refined using SHELXL-97 with anisotropic displacement factors for all non-hydrogen atoms.

Synthesis of [PPN][Cu(^{TMS}PS3)Cl] (1). $^{TMS}PS3H_3$ (115.4 mg, 0.20 mmol) was deprotonated by NaH (16.4 mg, 0.65 mmol) in THF (10 mL) for several hours under N_2. $[PPN]_2[Cu_2Cl_6]$ (282.2 mg, 0.199 mmol, or equimolar anhydrous $CuCl_2$ and PPNCl) was dissolved in 15 mL of CH_3CN. The THF solution of deprotonated ligand was filtrated through Celite to remove excess NaH, and subsequently transferred into the CH_3CN solution of $[PPN]_2[Cu_2Cl_6]$. The reaction solution was bubbled with O_2 for 1 h to improve the yield of **1**. The solvent of the resulting solution was removed by vacuum; the residue was redissolved with minimum amount of CH_3CN and filtrated. The same procedure was repeated with THF and CH_2Cl_2 sequentially. The CH_2Cl_2 filtrate was charged in vial(s) and crystallized by vapor diffusion with Et_2O at −10 °C. After the diffusion was completed, tawny supernatant was removed. Crystals were washed with Et_2O and air-dried; deep purple crystals were obtained by manual removal of cocrystallized white PPN^+ salt. Recrystallization of the crude was required to obtain complex **1** (58.5 mg, 24%). Yield of **1** is varied around 30−40% due to hemilability of chloride in solution as previous description. Anal. Calcd for $C_{63.5}H_{67}Cl_2CuNP_3S_3Si_3$ (**1**·0.5CH_2Cl_2): C, 60.91; H, 5.39; N, 1.12; S, 7.42. Found: C, 60.90; H, 5.66; N, 1.06; S, 7.23%. NMR spectra of **1** were recorded with additional PPNCl to suppress the dissociation of chloride. ^{1}H NMR (400 MHz, CD_3CN, δ): 7.69−7.63 (m, xs PPN), 7.62−7.53 (m, xs PPN), 7.52−7.44 (m, xs PPN with 3H of **1**), 6.98 (td, J = 7.4, 4.6 Hz, 3H), 6.66 (ddd, J = 12.1, 7.8, 1.3 Hz, 3H), 0.32 (s, 27H, TMS of **1**). ^{31}P NMR (162 MHz, CD_3CN, δ): 53.9, 20.8 (PPN). ^{13}C NMR (101 MHz, CD_3CN, δ): 161.8 (d, J = 15.2 Hz), 140.5 (d, J = 2.8 Hz), 139.6 (d, J = 11.2 Hz), 135.9 (d, J = 71.1 Hz), 134.7 (PPN), 133.3 (m, PPN), 132.1 (d, J = 7.6 Hz), 130.4 (m, PPN), 128.3 (d, J = 108.1 Hz, PPN), 122.8 (d, J = 10.8 Hz), −0.73 (TMS of **1**). HRMS-ESI (m/z): $[Cu(^{TMS}PS3)Cl]^-$ calcd for $C_{27}H_{36}ClCuPS_3Si_3$, 669.0009; found, 669.0007. UV−vis (CH_3CN) λ_{max}, nm (ε): 525 (8600), 730 (1600).

Synthesis of [PPN][Cu(^{TMS}PS3)(N_3)] (2). Complex **1** (57.9 mg, 0.046 mmol) was dissolved in 5 mL of CH_3CN, and excess NaN_3 (4.4 mg, 0.067 mmol) was subsequently added. The reaction mixture turned reddish brown within 1 h. The azide-bound complex **2** was obtained almost quantitatively after evaporation and recrystallization. Another way to synthesize **2** is following the general protocol for synthesizing **1** but adding excess NaN_3 right after O_2 bubbling in a one-pot fashion; up to 81% yield was achieved on a 0.2 mmol scale. Anal. Calcd for $C_{63}H_{66}CuN_4P_3S_3Si_3$: C, 62.22; H, 5.47; N, 4.61; S, 7.91. Found: C, 61.93; H, 5.55; N, 4.48; S, 7.63%. ^{1}H NMR (400 MHz, CD_3CN, δ): 7.69−7.63 (m, PPN), 7.62−7.53 (m, PPN), 7.52−7.43 (m, PPN with 3H of **2**), 7.00 (td, J = 7.5, 4.2 Hz, 3H), 6.74 (ddd, J = 12.0, 7.7, 1.4 Hz, 3H), 0.33 (s, 27H, TMS of **2**). ^{31}P NMR (162 MHz, CD_3CN, δ): 54.3, 20.8 (PPN). ^{13}C NMR (101 MHz, CD_3CN, δ): 161.5 (d, J = 15.1 Hz), 140.5 (d, J = 2.4 Hz), 139.6 (d, J = 11.2 Hz), 135.3 (d, J = 71.0 Hz), 134.7 (PPN), 133.3 (m, PPN), 132.4 (d, J = 7.0 Hz), 130.5 (m, PPN), 128.3 (d, J = 108.1 Hz, PPN), 123.1 (d, J = 10.4 Hz), −0.69 (TMS of **2**). IR (CH_3CN) $\bar{\nu}_{max}$: 2043s cm^{-1} (s, N_3). HRMS-ESI (m/z): $[Cu(^{TMS}PS3)(N_3)]^-$ calcd for $C_{27}H_{36}CuN_3PS_3Si_3$, 676.0413; found, 676.0413. UV−vis (CH_3CN) λ_{max}, nm (ε): 290 (24 000), 390 (6800), 515 (7800), 730 (2000).

Synthesis of [Cu(^{TMS}PS3)(DABCO)] (3). Complex **1** (79.5 mg, 0.063 mmol) was mixed with excess DABCO (16.0 mg, 0.142 mmol) in 10 mL of CH_3CN. The reaction mixture was stirred for several hours, and some brown precipitate appeared. The solvent of the reaction solution was evaporated, and the crude was redissolved using a minimum amount of THF. Then, Et_2O was added to the concentrated THF solution to precipitate PPNCl and some extra DABCO. The resulting solution was filtered for crystallization. Crystals of **3** were obtained via vapor diffusion by THF/Et_2O combination with a little additive benzene. ^{1}H NMR (400 MHz, C_6D_6, δ): 7.48 (ddd,, J = 7.0, 3.4, 1.6 Hz, 3H), 6.79 (ddd-like, J = 12.4, 7.7, 1.5 Hz, 3H), 6.74 (td-like, J = 7.5, 4.8 Hz, 3H), 0.47 (s, 27H, TMS of **3**). ^{31}P NMR (162 MHz, C_6D_6, δ): 41.9. ^{13}C NMR (101 MHz, C_6D_6, δ): 159.7 (d, J = 13.6 Hz), 140.3 (d, J = 2.6 Hz), 139.5 (d, J = 11.1 Hz), 135.1 (d, J = 73.8 Hz), 131.8 (d, J = 7.8 Hz), 123.2 (d, J = 11.3 Hz), 50.1 (DABCO), 47.4 (DABCO), −0.30 (TMS of **3**). HRMS−ESI (m/z): $[Cu(^{TMS}PS3)(DABCO) + H]^+$ calcd for $C_{33}H_{49}CuN_2PS_3Si_3$, 747.1394; found 746.1399. UV−vis (CH_3CN) λ_{max}, nm (ε): 490 (11 000), 700 (1800).

Ligand Exchange of 1 with NaSCN. Complex **1** was charged in a flask and dissolved in CH_3CN, followed by addition of excess NaSCN. The reaction mixture was stirred overnight for the ligand exchange of Cl^- in **1** to SCN^-. This exchange was also carried out in a one-pot fashion: Excess NaSCN was added into the preparation solution of **1** right after O_2 bubbling. Evaporation and recrystallization in the same manner as synthesis of **1**−**3** gave some purple crystals. ^{31}P NMR spectrum of the crystals showed two phosphorus-containing species coexist: **1** at 53.9 ppm and another species (**A**) at 48.0 ppm, along with a signal of PPN counterion at 20.8 ppm. These two components were also discriminated in ^{1}H and ^{13}C NMR. ^{1}H NMR (400 MHz, CD_3CN, δ): 7.69−7.62 (m, PPN), 7.62−7.38 (m, PPN with 3H of **1**/**A**), 7.05−6.94 (m, 3H of **1**/**A**), 6.69−6.63 (ddd-like, J = 12.5, 7.8, 1.3 Hz, 3H of **1**/**A**), 0.33−0.32 (27H of **1**/**A**). ^{13}C NMR (101 MHz, CD_3CN, δ): 161.7/161.4 (d, J = 15 Hz, **1**/**A**), 140.8/140.5 (d, J = 2.5 Hz, **A**/**1**), 139.6/139.2 (d, J = 11.3 Hz, **1**/**A**), 139.4 (SCN^- in **A**), 135.9 (d, J = 71.9 Hz, **1**)/135.5 (d, J = 72.9 Hz, **A**), 134.7 (PPN), 133.3 (m, PPN), 132.1 (d, J = 8.0 Hz, **1**/**A**), 130.4 (m, PPN), 128.3 (d, J = 108.1 Hz, PPN), 123.3 (d, J = 11.2 Hz, **A**)/122.8 (d, J = 10.8 Hz, **1**), −0.74/−0.79 (TMS of **1**/**A**). With a characteristic stretching peak for metal-bound SCN^- at 2104 cm^{-1}, the species **A** is assigned as [PPN][Cu(^{TMS}PS3)(NCS)], which is confirmed by high resolution mass as well. HRMS-ESI (m/z): $[Cu(^{TMS}PS3)(NCS)]^-$ calcd for $C_{28}H_{36}CuNPS_4Si_3$, 692.0072; found, 692.0072.

Ligand Affinity Measurement. Considering that the axial chloride of **1** exchanges with additional ligand (L) in an equilibrium manner as in eq 1, the relative affinity of L toward the [Cu(^{TMS}PS3)]

DOI: 10.1021/acs.inorgchem.5b00603
Inorg. Chem. 2015, 54, 5527−5533

moiety is represented by equilibrium constant K_{eq}. From the definition, K_{eq} can be expressed with the chemical components as in eq 2, where m and n, respectively, stand for the equivalence of Cl^- ion and incoming ligand; and Δ stands for the conversion ratio, the amount of [Cu(^{TMS}PS3)]−L within the whole copper species. Further, the conversion ratio is deduced as a function of m, n, and K_{eq} (eq 3). Hence the equilibrium constant is acquired by curve fitting of each titration isotherm with K_{eq} as a variable.

$$[Cu(^{TMS}PS3)]{-}Cl^- + L \rightleftharpoons [Cu(^{TMS}PS3)]{-}L + Cl^- \quad (1)$$

$$K_{eq} = \frac{\Delta(\Delta + m)}{(1 - \Delta)(n - \Delta)} \quad (2)$$

$$\Delta = \frac{((n+1)K_{eq} + m) - \sqrt{((n+1)K_{eq} + m)^2 - 4n(K_{eq} - 1)K_{eq}}}{2(K_{eq} - 1)} \quad (3)$$

The UV−vis titrations were carried out with **1** (1×10^{-4} M, 2.500 mL) and 5 or 10 equiv of PPNCl in CH_3CN. The excess Cl^- ion helped to suppress side exchange; better data were obtained for fitting. Stock solutions of ligands (L) were prepared at least 2 orders of magnitude more concentrated than the solution of **1** to minimize the dilution effect, but then, absorbance of UV−vis spectra needed to be adjusted by a dilution factor during analysis. Microsyringes were utilized to quantify the exact titration volume as well as the equivalence of ligands. After each portion of ligand added, the spectrum was monitored for a 5−10 min period to ensure the equilibrium was achieved. A final large amount of excess ligand was added in each titration to check that the completeness of ligand exchange occurred on the [Cu(^{TMS}PS3)] moiety. The conversion ratio at each step could be correctly calculated from spectral deconvolution.

Cu K-Edge Absorption Spectroscopy. X-ray absorption spectra were measured at the National Synchrotron Radiation Research Center (NSRRC, Taiwan), by BL17C1 wriggler beamline with a double-crystal Si(111) monochromator ($\Delta E/E \sim 2.2 \times 10^{-4}$). The Cu K-edge spectra of complexes **1**−**3** and $[PPN]_2[Cu_2Cl_6]$ were measured in transmission mode with their crystalline powder along with a reference Cu foil. Absorption was recorded by a gas-ionization detector under ambient conditions, scanned from 8.780 to 9.779 keV. Data analysis was conducted by utilize *IFEFFIT*-based *Demeter* package (version 0.9.20).[32] The energy in spectra was calibrated by setting the first inflection point of Cu foil at 8980.3 eV.[33]

Density Functional Theory Calculations. DFT calculations were carried using Gaussian 09 program, Revision D.01.[28] Initial geometry was derived from X-ray structure of **1**. Employing B3LYP hybrid functional[34] with pseudopotential for atoms within first coordination sphere (Cu: LANL2DZ; P, S, Cl: LANL08)[35−37] and 6-31G(d) basis functions for ligand backbone (H, C, Si), a singlet geometry was converged without any imaginary frequency. Jobs with spin state other than singlet failed or were halted because of their relatively high potential energy, which accords with the silence in EPR spectrum of **1**. Time-dependent DFT calculation with singlet−singlet transitions help to rationalize the UV−vis absorption of **1** (details in Supporting Information).

CONCLUSION

Employing the $^{TMS}PS3^{3-}$ chelator, the copper(III) center of **1**−**3** is stabilized under ambient conditions, and a series of TBP $[Cu^{III}(^{TMS}PS3)(L)]^{0/-}$ complexes hence can be synthesized via the Cl-bound intermediate **1**. The Cu(^{TMS}PS3) moiety is spontaneously formed by $^{TMS}PS3^{3-}$-triggered intramolecular disproportionation of hexachlorocuprate(II) precursor. Further characterizations reveal that the electron deficiency of the copper center in Cu(^{TMS}PS3) is highly compensated by the supporting ligand, which correlates to the hemilability of the axial chloride of **1** in solution. Preliminary studies shows the apical ligand (L) in $[Cu(^{TMS}PS3)(L)]^{0/-}$ is readily exchangeable and the affinity is not dominant by Coulombic effect but nucleophilicity of the apical ligand. Further derivatization is therefore untrammelled. These results not only help to elucidate the properties of TBP copper(III) species but also originate studies of high valent copper relevant to biological and catalytic systems.

ASSOCIATED CONTENT

Supporting Information

UV−vis, NMR, and HRMS spectra of **1**−**3**; EPR spectra of **1**−**2**; computational result of **1**; and crystallographic data of **1**−**3** in CIF format. These materials are available free of charge via the Internet at The Supporting Information is available free of charge on the ACS Publications website at DOI: 10.1021/acs.inorgchem.5b00603.

AUTHOR INFORMATION

Corresponding Author

*E-mail: wzlee@ntnu.edu.tw.

Notes

The authors declare no competing financial interest.

ACKNOWLEDGMENTS

This work is supported by the Ministry of Science and Technology of Taiwan (Grant 102-2113-M-003-007-MY3 to W.-Z.L.). We thank Dr. Jeng-Lung Chen and Dr. Jyh-Fu Lee at the National Synchrotron Radiation Research Center (NSRRC, Taiwan) for facilities and assistance in X-ray absorption measurements. We also thank Prof. Ming-Kang Tsai (National Taiwan Normal University) for advice about DFT calculations and the National Center for High-performance Computing (NCHC, Taiwan) for computer time and facilities.

REFERENCES

(1) Hickman, A. J.; Sanford, M. S. *Nature* **2012**, *484*, 177−185.
(2) Conde, A.; Vilella, L.; Balcells, D.; Díaz-Requejo, M. M.; Lledós, A.; Pérez, P. J. *J. Am. Chem. Soc.* **2013**, *135*, 3887−3896.
(3) Evano, G.; Jouvin, K.; Theunissen, C.; Guissart, C.; Laouiti, A.; Tresse, C.; Heimburger, J.; Bouhoute, Y.; Veillard, R.; Lecomte, M.; Nitelet, A.; Schweizer, S.; Blanchard, N.; Alayrac, C.; Gaumont, A.-C. *Chem. Commun.* **2014**, *50*, 10008−10018.
(4) Que, L., Jr.; Tolman, W. B. *Angew. Chem., Int. Ed.* **2002**, *41*, 1114−1137.
(5) *Copper-Oxygen Chemistry*; Karlin, K. D., Itoh, S., Eds.; John Wiley & Sons: New York, 2011.
(6) (a) Aboelella, N. W.; Lewis, E. A.; Reynolds, A. M.; Brennessel, W. W.; Cramer, C. J.; Tolman, W. B. *J. Am. Chem. Soc.* **2002**, *124*, 10660−10661. (b) Aboelella, N. W.; Kryatov, S. V.; Gherman, B. F.; Brennessel, W. W.; Young, V. G., Jr.; Sarangi, R.; Rybak-Akimova, E. V.; Hodgson, K. O.; Hedman, B.; Solomon, E. I.; Cramer, C. J.; Tolman, W. B. *J. Am. Chem. Soc.* **2004**, *126*, 16896−16911. (c) Reynolds, A. M.; Gherman, B. F.; Cramer, C. J.; Tolman, W. B. *Inorg. Chem.* **2005**, *44*, 6989−6997.
(7) (a) Fujisawa, K.; Tanaka, M.; Moro-oka, Y.; Kitajima, N. *J. Am. Chem. Soc.* **1994**, *116*, 12079−12080. (b) Würtele, C.; Gaoutchenova, E.; Harms, K.; Holthausen, M. C.; Sundermeyer, J.; Schindler, S. *Angew. Chem., Int. Ed.* **2006**, *45*, 3867−3869.
(8) (a) Kobayashi, Y.; Ohkubo, K.; Nomura, T.; Kubo, M.; Fujieda, N.; Sugimoto, H.; Fukuzumi, S.; Goto, K.; Ogura, T.; Itoh, S. *Eur. J. Inorg. Chem.* **2012**, 4574−4578. (b) Ginsbach, J. W.; Peterson, R. L.; Cowley, R. E.; Karlin, K. D.; Solomon, E. I. *Inorg. Chem.* **2013**, *52*, 12872−12874.
(9) (a) Sarangi, R.; Aboelella, N.; Fujisawa, K.; Tolman, W. B.; Hedman, B.; Hodgson, K. O.; Solomon, E. I. *J. Am. Chem. Soc.* **2006**,

DOI: 10.1021/acs.inorgchem.5b00603
Inorg. Chem. 2015, 54, 5527−5533

128, 8286−8296. (b) Cramer, C. J.; Tolman, W. B. *Acc. Chem. Res.* **2007**, *40*, 601−608.
(10) (a) Bertz, S. H.; Cope, S.; Murphy, M.; Ogle, C. A.; Taylor, B. J. *J. Am. Chem. Soc.* **2007**, *129*, 7208−7209. (b) Bertz, S. H.; Cope, S.; Dorton, D.; Murphy, M.; Ogle, C. A. *Angew. Chem., Int. Ed.* **2007**, *46*, 7082−7085. (c) Bartholomew, E. R.; Bertz, S. H.; Cope, S.; Dorton, D. C.; Murphy, M.; Ogle, C. A. *Chem. Commun.* **2008**, 1176−1177. (d) Bertz, S. H.; Murphy, M. D.; Ogle, C. A.; Thomas, A. A. *Chem. Commun.* **2010**, *46*, 1255−1256.
(11) Gschwind, R. M. *Chem. Rev.* **2008**, *108*, 3029−3053.
(12) (a) Casitas, A.; Ribas, X. *Chem. Sci.* **2013**, *4*, 2301−2318. (b) Huffman, L. M.; Casitas, A.; Font, M.; Canta, M.; Costas, M.; Ribas, X.; Stahl, S. S. *Chem.—Eur. J.* **2011**, *17*, 10643−10650.
(13) (a) Casitas, A.; King, A. E.; Parella, T.; Costas, M.; Stahl, S. S.; Ribas, X. *Chem. Sci.* **2010**, *1*, 326−330. (b) Ribas, X.; Xifra, R.; Parella, T.; Poater, A.; Solà, M.; Llobet, A. *Angew. Chem., Int. Ed.* **2002**, *41*, 2991−2994. (c) King, A. E.; Huffman, L. M.; Casitas, A.; Costas, M.; Ribas, X.; Stahl, S. S. *J. Am. Chem. Soc.* **2010**, *132*, 12068−12073. (d) Rovira, M.; Font, M.; Acuña-Parés, F.; Parella, T.; Luis, J. M.; Lloret-Fillol, J.; Ribas, X. *Chem.—Eur. J.* **2014**, *20*, 10005−10010.
(14) (a) Yao, B.; Wang, D.-X.; Huang, Z.-T.; Wang, M.-X. *Chem. Commun.* **2009**, 2899−2901. (b) Zhang, H.; Zhao, L.; Wang, D.-X.; Wang, M.-X. *Org. Lett.* **2013**, *15*, 3836−3839. (c) Zhang, H.; Yao, B.; Zhao, L.; Wang, D.-X.; Xu, B.-Q.; Wang, M.-X. *J. Am. Chem. Soc.* **2014**, *111*, 6326−6332.
(15) (a) Furuta, H.; Maeda, H.; Osuka, A. *J. Am. Chem. Soc.* **2000**, *122*, 803−807. (b) Maeda, H.; Ishikawa, Y.; Matsuda, T.; Osuka, A.; Furuta, H. *J. Am. Chem. Soc.* **2003**, *125*, 11822−11823. (c) Maeda, H.; Osuka, A.; Furuta, H. *J. Am. Chem. Soc.* **2003**, *125*, 15690−15691.
(16) Fritsky, I. O.; Kozłowski, H.; Kanderal, O. M.; Haukka, M.; Świątek-Kozłowska, J.; Gumienna-Kontecka, E.; Meyer, F. *Chem. Commun.* **2006**, 4125−4127.
(17) (a) Coucouvanis, D.; The Chemistry of the Dithioacid and 1,1-Dithiolate Complexes, 1968−1977. In *Progress in Inorganic Chemistry*; Lippard, S. J., Ed.; John Wiley & Sons: New York, 1979; Vol. *26*, pp 324−330. (b) Kanatzidis, M. G.; Baenziger, N. C.; Coucouvanis, D. *Inorg. Chem.* **1985**, *24*, 2680−2683.
(18) Vicente, J.; González-Herrero, P.; García-Sánchez, Y.; Jones, P. G.; Bautista, D. *Eur. J. Inorg. Chem.* **2006**, 115−126.
(19) Santo, R.; Miyamoto, R.; Tanaka, R.; Nishioka, T.; Sato, K.; Toyota, K.; Obata, M.; Yano, S.; Kinoshita, I.; Ichimura, A.; Takui, T. *Angew. Chem., Int. Ed.* **2006**, *45*, 7611−7614.
(20) Romine, A. M.; Nebra, N.; Konovalov, A. I.; Martin, E.; Benet-Buchholz, J.; Grushin, V. V. *Angew. Chem., Int. Ed.* **2015**, *54*, 2745−2749.
(21) Block, E.; Ofori-Okai, G.; Zubieta, J. *J. Am. Chem. Soc.* **1989**, *111*, 2327−2329.
(22) Chu, W.-C.; Wu, C.-C.; Hsu, H.-F. *Inorg. Chem.* **2006**, *45*, 3164−3166.
(23) Lee, C.-M.; Chuo, C.-H.; Chen, C.-H.; Hu, C.-C.; Chiang, M.-H.; Tseng, Y.-J.; Hu, C.-H.; Lee, G.-H. *Angew. Chem., Int. Ed.* **2012**, *51*, 5427−5430.
(24) (a) Niemoth-Anderson, J. D.; Clark, K. A.; George, T. A.; Ross, C. R., II. *J. Am. Chem. Soc.* **2000**, *122*, 3977−3978. (b) Clark, K. A.; George, T. A. *Inorg. Chem.* **2005**, *44*, 416−422.
(25) (a) Lee, C.-M.; Chuang, Y.-L.; Chiang, C.-Y.; Lee, G.-H.; Liaw, W.-F. *Inorg. Chem.* **2006**, *45*, 10895−10904. (b) Lee, C.-M.; Chen, C.-H.; Liao, F.-X.; Hu, C.-H.; Lee, G.-H. *J. Am. Chem. Soc.* **2010**, *132*, 9256−9258.
(26) (a) Textor, M.; Dubler, E.; Oswald, H. R. *Inorg. Chem.* **1974**, *13*, 1361−1365. (b) Hasselgren, C.; Jagner, S.; Dance, I. *Chem.—Eur. J.* **2002**, *8*, 1270−1278.
(27) Barbier, J.; Hugel, R. P.; Kappenstein, C. *Inorg. Chim. Acta* **1983**, *77*, L117−L118.
(28) Frisch, M. J.; Trucks, G. W.; Schlegel, H. B.; Scuseria, G. E.; Robb, M. A.; Cheeseman, J. R.; Scalmani, G.; Barone, V.; Mennucci, B.; Petersson, G. A.; Nakatsuji, H.; Caricato, M.; Li, X.; Hratchian, H. P.; Izmaylov, A. F.; Bloino, J.; Zheng, G.; Sonnenberg, J. L.; Hada, M.; Ehara, M.; Toyota, K.; Fukuda, R.; Hasegawa, J.; Ishida, M.; Nakajima, T.; Honda, Y.; Kitao, O.; Nakai, H.; Vreven, T.; Montgomery, J. A., Jr.; Peralta, J. E.; Ogliaro, F.; Bearpark, M.; Heyd, J. J.; Brothers, E.; Kudin, K. N.; Staroverov, V. N.; Keith, T.; Kobayashi, R.; Normand, J.; Raghavachari, K.; Rendell, A.; Burant, J. C.; Iyengar, S. S.; Tomasi, J.; Cossi, M.; Rega, N.; Millam, J. M.; Klene, M.; Knox, J. E.; Cross, J. B.; Bakken, V.; Adamo, C.; Jaramillo, J.; Gomperts, R.; Stratmann, R. E.; Yazyev, O.; Austin, A. J.; Cammi, R.; Pomelli, C.; Ochterski, J. W.; Martin, R. L.; Morokuma, K.; Zakrzewski, V. G.; Voth, G. A.; Salvador, P.; Dannenberg, J. J.; Dapprich, S.; Daniels, A. D.; Farkas, O.; Foresman, J. B.; Ortiz, J. V.; Cioslowski, J.; Fox, D. J. *Gaussian 09, Revision D.01*; Gaussian, Inc.: Wallingford, CT, 2013.
(29) (a) Kau, L.-S.; Spira-Solomon, D. J.; Penner-Hahn, J. E.; Hodgson, K. O.; Solomon, E. I. *J. Am. Chem. Soc.* **1987**, *109*, 6433−6442. (b) DuBois, J. L.; Mukherjee, P.; Collier, A. M.; Mayer, J. M.; Solomon, E. I.; Hedman, B.; Stack, T. D. P.; Hodgson, K. O. *J. Am. Chem. Soc.* **1997**, *119*, 8578−8579. (c) DuBois, J. L.; Mukherjee, P.; Stack, T. D. P.; Hedman, B.; Solomon, E. I.; Hodgson, K. O. *J. Am. Chem. Soc.* **2000**, *122*, 5775−5787.
(30) Sarangi, R.; George, S. D.; Rudd, D. J.; Szilagyi, R. K.; Ribas, X.; Rovira, C.; Almeida, M.; Hodgson, K. O.; Hedman, B.; Solomon, E. I. *J. Am. Chem. Soc.* **2007**, *129*, 2316−2326.
(31) Hocking, R. K.; Solomon, E. I. Ligand Field and Molecular Orbital Theories of Transition Metal X-ray Absorption Edge Transitions. In *Molecular Electronic Structures of Transition Metal Complexes I*; Mingos, D. M. P., Day, P., Dahl, J. P., Eds.; Springer-Verlag: Berlin, 2011; pp 155−184.
(32) Ravel, B.; Newville, M. *J. Synchrotron Radiat.* **2005**, *12*, 537−541. *Demeter* is available online: http://bruceravel.github.io/demeter/.
(33) Bearden, J. A.; Burr, A. F. *Rev. Mod. Phys.* **1967**, *39*, 125−142.
(34) (a) Becke, A. D. *Phys. Rev. A* **1988**, *38*, 3098−3100. (b) Becke, A. D. *J. Chem. Phys.* **1993**, *98*, 5648−5652. (c) Lee, C. T.; Yang, W. T.; Parr, R. G. *Phys. Rev. B: Condens. Matter Mater. Phys.* **1988**, *37*, 785−789.
(35) *Basis Set Exchange*; https://bse.pnl.gov/bse/portal/.
(36) (a) Feller, D. *J. Comput. Chem.* **1996**, *17*, 1571−1586. (b) Schuchardt, K. L.; Didier, B. T.; Elsethagen, T.; Sun, L.; Gurumoorthi, V.; Chase, J.; Li, J.; Windus, T. L. *J. Chem. Inf. Model.* **2007**, *47*, 1045−1052.
(37) (a) Hay, P. J.; Wadt, W. R. *J. Chem. Phys.* **1985**, *82*, 270−283. (b) Hay, P. J.; Wadt, W. R. *J. Chem. Phys.* **1985**, *82*, 299−310. (c) Check, C. E.; Faust, T. O.; Bailey, J. M.; Wright, B. J.; Gilbert, T. M.; Sunderlin, L. S. *J. Phys. Chem. A* **2001**, *105*, 8111−8116.

DOI: 10.1021/acs.inorgchem.5b00603
Inorg. Chem. 2015, 54, 5527−5533